Cyclic thermal signature in a global MHD simulation of solar convection

Jean-Francois Cossette[1] and Paul Charbonneau[1]
Physics Department, Université de Montréal, Montréal, Canada

Piotr K. Smolarkiewicz[2]
European Centre for Medium-Range Weather Forecasts, Reading, UK

ABSTRACT

Global magnetohydrodynamical simulations of the solar convection zone have recently achieved cyclic large-scale axisymmetric magnetic fields undergoing polarity reversals on a decadal time scale (Beaudoin et al. 2013; Racine et al. 2011; Ghizaru et al. 2010). In this Letter, we show that these simulations also display a thermal convective luminosity that varies in-phase with the magnetic cycle, and trace this modulation to deep-seated magnetically-mediated changes in convective flow patterns. Within the context of the ongoing debate on the physical origin of the observed 11-year variations in total solar irradiance, such a signature supports the thesis according to which all, or part of the variations on decadal time scales and longer could be attributed to a global modulation of the Sun's internal thermal structure by magnetic activity.

Subject headings: Total solar irradiance, solar activity, MHD, solar convection

1. IRRADIANCE VARIATIONS AND THE SOLAR DYNAMO

Total solar irradiance (TSI) has been measured almost continuously by earth-orbiting satellites for more than three decades and is now known to vary on time scales from minutes to days and months as well as on the longer time scale of the 11-year solar-cycle; see (Kopp & Lean 2011; Fröhlich & Lean 2004). Perhaps the most striking feature that emerges from observational measurements is the slight increase of the TSI ($\approx 0.1\%$) at solar activity maxima relative to its value at solar minima. Models that include the contributions of sunspots, faculae and magnetic network to reconstruct irradiance time series succeed very well at reproducing the observations on the short, intra-cycle time scales (e.g. shorter than a year). So far, however, pin-pointing the source of the longer decadal fluctuations has remained the subject of controversy. In particular, one school of thought argues that surface magnetism alone is sufficient to explain the entire TSI variance (Foukal et al. 2006; Lean et al. 1998); whereas, the other emphasizes the effect of a global modulation of thermal structure by magnetic activity (Sofia & Li 2006; Li et al. 2003). Within a broader context, establishing the contribution of a global thermal modulation to TSI variability relative to that of emerging magnetic flux structures at the solar surface is valuable for quantifying the coupling between periods of quiet surface magnetism and the Earth's climate, such as the postulated relationship between the Maunder Minimum and the Little Ice Age (Foukal et al. 2011). It is the potential for the occurence of such changes which we consider in this Letter.

In principle, magnetically-modulated global structural changes could take place through the action of the Lorentz force onto the large-scale heat-carrying convective flows, which would then affect temperature and pressure conditions throughout the solar interior. Evidence for such a hypothetical mechanism is partly supported by helioseismic observations that show a positive cor-

relation between low-degree p-mode acoustic oscillations frequencies and the TSI cycle, as well as recent evidence for a long-term trend in the TSI record that is not seen in indicators of surface magnetism; (Fröhlich 2013; Bhatnagar et al. 1999; Woodward 1987). Other observations document possible variations of the surface temperature and changes in the solar diameter; (Harder et al. 2009; Thuillier et al. 2005; Gray & Livingston 1997; Kuhn et al. 1988).

Notably, structural models of the Sun have shown that by incorporating the effect of a magnetically-modulated turbulent mechanism into the 1D stellar structure equations, it is possible to reproduce the time-dependence of the observed p-mode frequency oscillations along with the expected variations in solar radius, luminosity and effective temperature (Sofia & Li 2006; Li et al. 2003). However, these models relied upon an ad-hoc parametrization of the alleged process and therefore solving the full set of equations governing the self-consistent evolution of the solar plasma remains necessary to obtain a complete physical picture of the mechanism at the origin of the modulation.

Fortunately, global magnetohydrodynamical (MHD) simulations of the solar convection zone (SCZ) have recently been able to produce regular, solar-like magnetic cycles undergoing hemispheric polarity reversals on a decadal time scale (Beaudoin et al. 2013; Racine et al. 2011; Käpylä & al. 2010; Ghizaru et al. 2010), and therefore offer the opportunity for the search and investigation of potential global structural changes. In this paper we report on a global MHD simulation of the SCZ that shows a modulation of the convective heat flux by a solar-like cyclic large-scale magnetic field. In section 2 we briefly document the physical setup of our experiment and describe the main results. In section 3, we further explore the simulation data in search of plausible physical mechanisms that could explain the observed thermodynamic signal and we conclude the paper in section 4 by pointing out a few possible observational signatures.

2. RESULTS: MODULATION OF THE CONVECTIVE HEAT FLUX

We solve the anelastic form of the ideal MHD equations for momentum, potential temperature fluctuations (tantamount to fluctuations of specific entropy) and magnetic induction inside a thick spherical shell of electrically-conducting fluid extending from $r = 0.602R_\odot$ to $r = 0.96R_\odot$ in radius, rotating at the solar rate $\Omega_\odot = 2.69\times10^{-6}$rad s^{-1} and spanning 3.4 density scale-heights. Rather than forcing convection by applying large-amplitude solar heating and cooling fluxes at bottom and top boundaries, as it is customary in simulations of stellar convection, a Newtonian-cooling term in the potential temperature equation damps naturally-occuring departures from an ambient state representative of the current-day Sun on a user-defined time scale τ. The ambient state is subadiabatically-stratified in the lower portion of the shell corresponding to the radiative interior ($0.602R_\odot \leq r \leq 0.71R_\odot$) and is weakly superadiabatic in the range associated with the bulk of the convective layer ($0.71R_\odot \leq r \leq 0.96R_\odot$). This approach has lead to convective dynamo solutions exhibiting a number of solar-like properties, the most prominent of which is a large-scale axisymmetric magnetic field component undergoing polarity reversals about the equatorial plane on a 40-year time scale; see the following publications for an in-depth exploration of various solar-like features found to this day: (Beaudoin et al. 2013; Racine et al. 2011; Ghizaru et al. 2010). Solutions are generated with the MHD-extended version of the EULAG model (Smolarkiewicz & Charbonneau 2013), an all-scale high-performance hydrodynamical code used primarily in atmospheric and climate research (Prusa et al. 2008). We hereby focus on a recent simulation covering 32 magnetic polarity reversals (similar in design and the resulting flow regime to the one presented in Ghizaru et al. 2010) in which global structural changes have been observed.

Convection and Newtonian cooling are the dominant modes of thermal energy transport in the unstable layer and nearly cancel each other out to yield a quasi-stationnary turbulent state, with the contribution from radiation being negligible. The means by which we quantify the efficiency of

convective energy transfer is the convective heat flux, or enthalpy flux, which in the anelastic approximation is given by $F \equiv c_p \rho_o u_r \widetilde{T}$, where c_p is the specific heat at constant pressure, ρ_o is the density associated with the reference state of the approximation, u_r is the vertical component of the velocity and $\widetilde{T}$ is the temperature perturbation with respect to the mean horizontal state. The convective luminosity is the integrated flux F over a spherical surface $L_{\rm cv} \equiv \int F \, d\sigma$.

The top and bottom panels of figure 1 show, respectively, a snapshot of F in a Mollweide projection (longitude vs latidude) at $r = 0.87 R_\odot$ and a correlation plot of F versus u_r at the same height, with numbers indicating the fraction of points contained in each quadrant. The two dashed lines in the top plot delimit, respectively, the inside and the outside regions (hereafter, the mid/high latitudes) of the equatorial band comprised between the latitude circles $\theta = \pm 30^{\rm o}$. Notably, the flux at the mid/high latitudes is spatially very intermittent, despite the low grid resolution of the experiment ($N_\phi \times N_\theta \times N_r = 128 \times 64 \times 47$), where N_ϕ, N_θ and N_r stand for, respectively, the number of grid points in the longitudinal, latitudinal and radial directions. In particular, the strongest heat fluxes (i.e. $F \geq 1.5 \times 10^7$ W$\cdot$m^{-2}) appear in the form of localized concentrations or 'hot spots'; whereas, cooling regions (i.e. $F < 0$) correspond to the weaker fluxes that are interspersed among the latter. By contrast, the equatorial band is dominated by North-south positive and negative flux lanes, which are the thermal signature of the convective modes commonly known as 'banana cells' and are characteristic of flows in a rotating spherical shell (see Miesch and Toomre 2009 for an in-depth discussion of global convective dynamics). The bottom plot shows that approximately 70% of upflows and downflows contribute to positive fluxes, while the remaining 30% is responsible for cooling by fluid entrainment; a landmark of flows operating in a highly turbulent regime. Here the asymmetry between distributions associated with $u_r > 0$ and $u_r < 0$ can be traced back to the pattern of broad upflows and narrow downflow lanes typical of thermal convection in a density-stratified environnement; see, e.g., fig. 1 of (Ghizaru et al. 2010) and fig. 2 of (Miesch & Toomre 2009).

Figure 2 displays time-latitude plots of the zonally-averaged toroidal component of the mag-

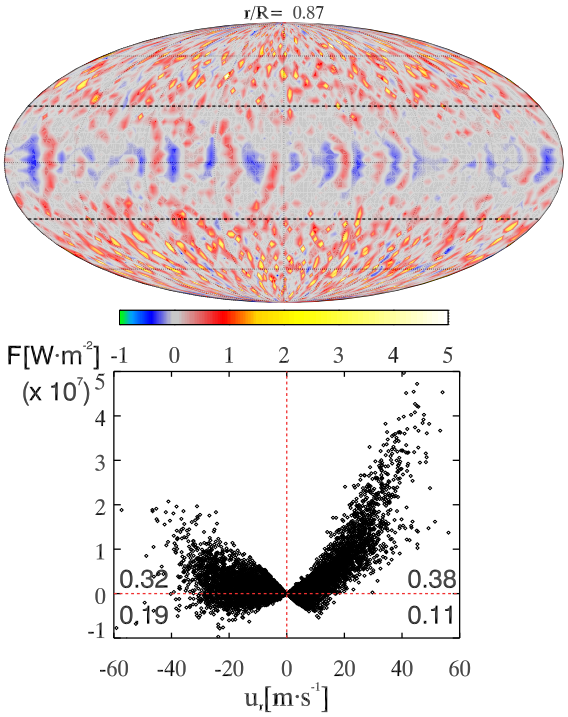

Fig. 1.— A simulation snapshot: Mollweide projection of the convective heat flux $F(\theta, \phi)$ at $r = 0.87 R_\odot$ (top) and its correlation with the vertical flow velocity at the same height (bottom). Each diamond corresponds to the value of F at a grid point on the spherical shell, and the numbers give the fraction of grid point values appearing in each quadrant.

netic field (top panel) and zonally-averaged deviation about the temporal mean of F at $r = 0.87R_\odot$ (bottom) for a segment of the simulation spanning slightly more than 150 years. The axisymmetric toroidal field is clearly antisymmetric about the equator and is split into a large-scale component at mid/high latitudes reversing polarities on a period varying between 30 and 40 years and another flux concentration located in the equatorial band evincing a shorter, 3 to 5 year oscillatory signal. Interestingly, helioseismic frequency analysis and indicators of geomagnetic activity suggest the presence of a short-term magnetic cycle operating inside the Sun, in addition to the well-known 11-year signal (Fletcher & al. 2010; Mursula et al. 2003). The bottom plot shows the global thermal modulation. In particular, at mid/high latitudes, the convective heat flux is temporally well correlated with the absolute value of the zonally-averaged toroidal magnetic field. Likewise, the signature of the short-term magnetic cycle can be seen in the flux comprised within the equatorial band, although it appears to be in anti-phase with the flux variation at the mid/high latitudes. Here, however, we postpone a thorough discussion of the short-term magnetic signal to a future publication and focus on changes related to the long-term cycle.

The top panel of fig. 3 displays histories of both the unstable layer's normalized total magnetic energy $E_m^\star \equiv E_m / \max(E_m)$ (black curve) and temporal perturbation of the normalized convective luminosity $\Delta L_{\rm cv}^\star \equiv (L_{\rm cv} - \bar{L}_{\rm cv})/\bar{L}_{\rm cv}$ at $r = 0.87R_\odot$ (red curve) and its 5-year running mean (yellow curve), where the maximum of magnetic energy is taken over the full time-sequence of the simulation and $\bar{L}_{\rm cv}$ is the time-averaged convective luminosity. Thus, the combination of the mid/high latitudes in-phase flux modulation and the equatorial band's signal gives a total convective flux variation that has the same phase as E_m. Its amplitude is of the order of 10% of $\bar{L}_{\rm cv}$, which itself only reaches 3% of the true solar luminosity $L_\odot$ at this given height, thereby yielding a modulation of amplitude $0.003L_\odot$. Although the amplitude of the modulation is comparable to that of the actual decadal TSI fluctuations, it must be kept in mind that this specific simulation is quite subluminous, with $L_{\rm cv}$ peaking at $\approx 0.1L_\odot$ at mid-depth of the domain. We shall comment further on this issue in section 4. Nevertheless, the sign of the correlation between $E_m^\star$ and $\Delta L_{\rm cv}^\star$ is positive ($r = +0.63$) and therefore consistent with an increase of TSI at solar maxima, as shown by the bottom panel, in which $\Delta L_{\rm cv}^\star$ is plotted as a function of $E_m^\star$. Notably, the scattering of points along the vertical axis can be attributed to the influence of the short-term magnetic cycle on the total convective luminosity. The fact that convective heat transport correlates positively with magnetic activity forcibly points to an intricate interplay between the flow and magnetic field topologies, since the presence of a magnetic field generally tends to inhibit, rather than enhance, the flow of an electrically conducting fluid, at least in the parameter regime relevant to solar interior conditions.

3. THE HUNT FOR THE PHYSICAL MECHANISM

As a first step towards the identification of the physical mechanism causing the observed modulation, we shall examine how strongly the convective flux at each grid point is modulated by the magnetic field. The top panel of figure 4 shows cumulative convective heat flux PDFs corresponding to, respectively, every minima (black continuous curve) and maxima (red dashed curve) of the simulation for the spherical surface located at $r = 0.87R_\odot$; cf. fig. 1. Observe that at peak time of the magnetic cycle, the amount of flux values corresponding to the hot spots increases with respect to its value at minimum time; whereas, the opposite phenomenon characterizes the negative flux values. The bulk of the positive flux distribution (i.e. $0 \leq F < 1.5 \times 10^7$ W $\cdot$ m^{-2}), on the other hand, shows no obvious change. To substantiate this, we have computed the correlation coefficient of the time sequence of each of the convective heat flux PDF's histogram bins with the time series of E_m for grid points on the full spherical shell (black continuous curve), the equatorial band (black dotted curve) and the mid/high latitudes (black dashed curve) and plotted the result in the bottom panel of fig. 4. Each bin contributes to some fraction of the total convective luminosity variation (cf. fig. 3), and red curves display their correlation with E_m. The correlation analysis confirms what could already be inferred from the cumulative PDFs, namely, that

there is a significant modulation of hot spot and negative flux populations by the magnetic cycle. Notably, the strong anti-correlation ($r \approx -0.6$) of the mid/high latitudes negative fluxes with E_m is the sign of a pronounced diminution of fluid entrainment at peak cycle time, which could be due to the suppression of turbulence by the intensification of the magnetic field. The bulk of the positive flux distribution does show a weak positive correlation with E_m, even though this change cannot be easily detected in the minima-maxima PDFs. Interestingly, this fluctuation translates into a decrease of the luminosity at cycle maximum, as shown by the anti-correlation with E_m near $F = 0$, and therefore implies a corresponding decrease of the filling factor of the associated flux regions. The means and variances of the luminosity variations implied by hot spots, elements from the bulk of the positive flux distribution and negative flux elements are, respectively, as expressed in terms of fractions of $\bar{L}_{\rm cv}$: (0.320; 0.039), (0.781; 0.024) and (−0.102; 0.007). The PDF of vertical velocities (not shown), on the other hand, is invariant with respect to magnetic energy and therefore implies that the action of the Lorentz force on the flow is not simply a straightforward suppression of buoyancy-driven flows by the magnetic field, which again suggests that the interplay between flow and field topologies is magnetohydrodynamically complex.

4. REMARKS

We have presented a basic analysis of a global MHD simulation of solar convection evincing a modulation of thermal structure by regular, solar-like, large-scale cyclic magnetic fields undergoing polarity reversals. Most importantly, the convective luminosity correlates positively with the magnetic cycle, which is consistent with the enhanced value of the TSI observed at solar maxima. The time analysis of the distribution of convective heat fluxes on a spherical surface allows to classify each flow feature according to the size of its contribution to the variance of the luminosity modulation; the most important effect being associated with the intense and localized positive flux elements known as hot spots, followed by a luminosity deficit coming from the bulk of the positive flux distribution, and a positive contribution due to a diminution of cooling via fluid entrainment. The latter may be attributed, for instance, to the suppression of turbulence by the enhanced magnetic field; whereas, the other two could be interpreted as manifestations of the flow's response to the modulation of turbulent entrainment by the cycle (recall the strong anti-correlation $r \approx -0.6$) while simultaneously satisfying the constraint of mass conservation and energy transport requirement imposed by the thermal forcing of the system. If such a speculative mechanism turned out to be real, it could well explain the weaker correlation of positive flux values with magnetic energy.

We have carried out our analysis of the flux variation at the given height $0.87R_\odot$, and find that the amplitude of the luminosity fluctuations implied by the modulation at this specific level is of the order of 0.3% of the true solar luminosity. However, the mean convective luminosity at this spherical shell is only of the order of $0.03L_\odot$ and the fact that our domain stops below the photosphere limits the type of comparisons that can be made with respect to the real Sun. For instance, the amplitude of the TSI variation implied by the global modulation may vary depending upon the subphotospheric layers' ability to store/release the heat flowing up from below as a result of the deep-seated flux signal (Foukal et al. 2006). Moreover, the use of an impenetrable velocity boundary condition at the top of our model, a common feature of global MHD simulations, suppresses convective motions in the outer layers and therefore prevents one from making accurate predictions as to potential impacts of the flux modulation on the upper SCZ's dynamics. Nevertheless, our observation of a positive correlation between convective energy transport efficiency and magnetic energy suggests that magnetically-modulated global structural changes could contribute to an enhancement of the TSI at peak cycle time. A quantitative estimate of the corresponding amplitude contribution will require further modeling of the upper SCZ's physical connection to the photosphere as well as carrying out a similar analysis at higher luminosity.

We are currently engaged in a detailed analysis of the modulation and its underlying physical mechanism, briefly discussed in this Letter. The overarching aim is to assess the implications that these results might have for the existence of activity cycle-driven structural changes inside

the Sun, and predict potential observational signatures. In this respect, the results presented here already indicate that the response of the convective flux to the magnetic activity cycle shows a significant latitudinal dependency, which could translate in cyclic variations of the surface pole-to-equator temperature contrast (viz. Rast et al. 2008; Kuhn et al. 1988), and/or asphericity of the solar photosphere (Thuillier et al. 2005).

Comments from an anonymous referee helped to improve the presentation. The numerical simulations reported in this paper were carried out primarily on the computing facilities of Calcul Québec, a member of the Compute Canada consortium. This work is supported by Canada's Foundation for Innovation, Natural Sciences and Engineering Research Chair program and Discovery Grant program (PC), and the NSERC Graduate Fellowship Program (JFC). PKS is supported by the European Research Council under the European Union's Seventh Framework Programme (FP7/2012/ERC Grant agreement No. 320375).

REFERENCES

Beaudoin, P., Charbonneau, P., Racine, E., & Smolarkiewicz, P. K. 2013, Sol. Phys., 282, 335

Bhatnagar, A., Jain, K., & Tripathy, S. C. 1999, ApJ, 521, 885

Fletcher, S. T., Broomhall, A.-M., Salabert, D., Basu, S., Chaplin, W. J., Elsworth, Y., Garcia, R. A. & New, R. 2010, ApJ, 718, L19

Foukal, P., Ortiz, A., & Schnerr, R. 2011, ApJ, 733, L38

Foukal, P., Fröhlich, C., Spruit, H., & Wigley, T. M. L. 2006, Nature, 443, 161

Fröhlich, C. 2013, Space Sci. Rev., 176, 237

Fröhlich, C., Lean, J. 2004, Astron. Astrophys. Rev., 12, 273

Ghizaru M., Charbonneau P., & Smolarkiewicz, P. K. 2010, ApJ, 715, L133

Gray, D. F., & Livingston, W. C. 1997, ApJ, 474, 802

Harder, J. W., Fontenla, J. M., Pilewskie, P., Richard, E. C., & Woods, T. N. 2009, Geophys. Res. Lett., 36, L07801

Käpylä, P. J., Korpi, M. J., Brandenburg, A., Mitra, D., & Tavakol, R. 2010, Astron. Nachr., 331, 73

Kopp, G., & Lean, J.L. 2011, Geophys. Res. Lett., 38, L01706

Kuhn, J. R., Libbrecht, K. G., & Dicke, R. H. 1988, Science, 242, 908

Lean, J. L., Cook, J., Marquette, W., & Johannesson, A. 1998, ApJ, 492, 390

Li, L. H., Basu, S., Sofia, S., Robinson, F. J., Demarque, P., & Guenther, D. B. 2003, ApJ, 591, 1267

Miesch, M. S., & Toomre, J. 2009, Annu. Rev. Fluid Mech. 41, 317

Mursula, K., Zieger, B., & Vilppola, J.H. 2003, Sol. Phys. 212, 201

Prusa, J. M., Smolarkiewicz, P. K., & Wyszogrodzki, A. A. 2008, Comput. Fluids, 37, 1193

Racine, E., Charbonneau, P., Ghizaru, M., Bouchat, A., & Smolarkiewicz, P. K. 2011, ApJ, 735, 46

Rast, M. P., Ortiz, A., & Meisner, R. W. 2008, ApJ, 673, 1209

Smolarkiewicz, P. K., & Charbonneau, P. 2013, J. Comput. Phys., 236, 608

Sofia, S., & Li, L. H. 2006, Mem. S. A. It., 76, 768

Thuillier, G., Sofia, S., & Haberreiter, M. 2005, Adv. Space. Res., 35, 329

Woodward, M. F. 1987, Sol. Phys., 114, 21

This 2-column preprint was prepared with the AAS LaTeX macros v5.2.

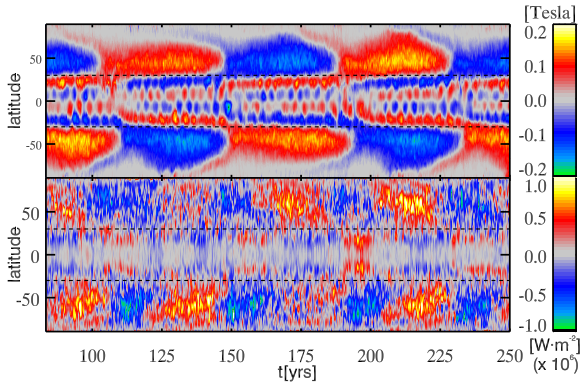

Fig. 2.— Temporal evolution: Zonally-averaged toroidal component of the magnetic field (top) and zonally-averaged deviation of the convective heat flux F (bottom) at $r = 0.87R_\odot$. At mid/high latitudes, the absolute value of the zonally-averaged toroidal field has a period and phase comparable to that of the flux variation.

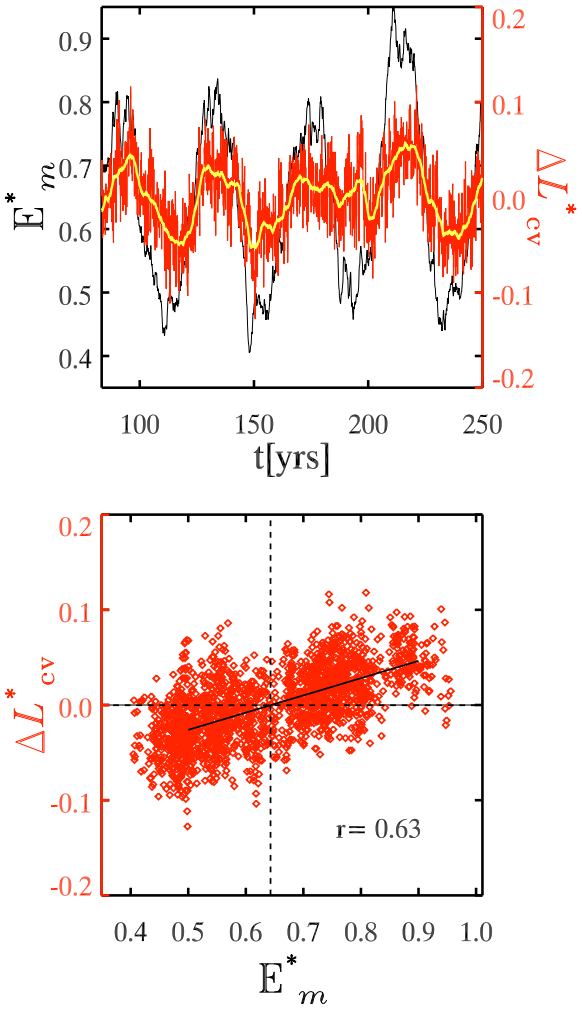

Fig. 3.— Top: Histories of normalized total magnetic energy (black curve) and temporal perturbation of the normalized convective luminosity (red curve) with its 5-year running mean (yellow curve). Bottom: Correlation between the temporal perturbation of convective luminosity and magnetic energy.

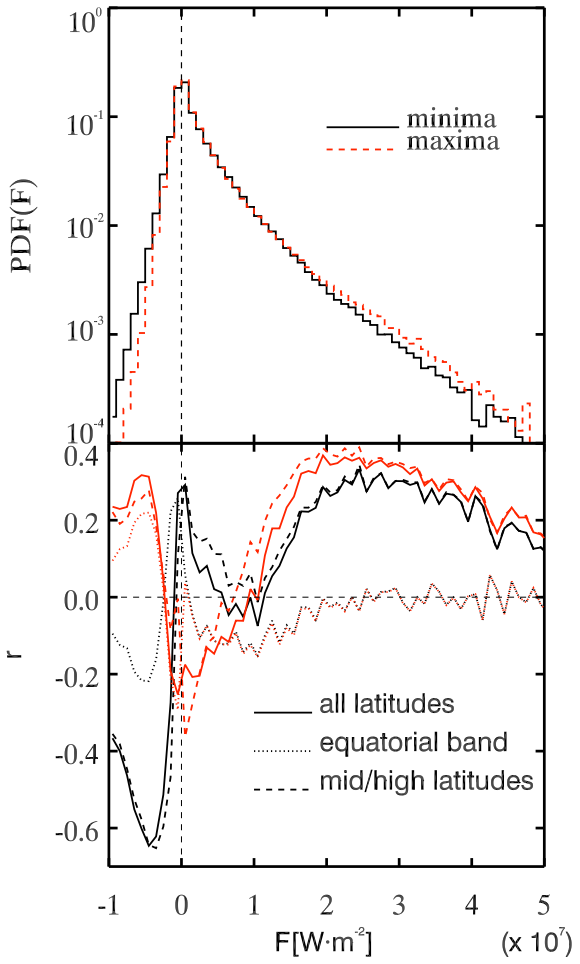

Fig. 4.— Top: Cumulative convective heat flux PDFs corresponding to, respectively, every minima (black continuous curve) and maxima (red dashed curve) of the simulation at grid points located at $r = 0.87R_{\odot}$. Here, maxima and minima are defined as extremal points in time of magnetic energy. Bottom: The black curves show the correlation coefficient of each bin of the convective heat flux's PDF with the time series of total magnetic energy for regions consisting of the full spherical shell (solid curve), the equatorial band (dotted curve) and the mid/high latitudes (dashed curve). Red curves display the correlation coefficient of each bin's associated luminosity input variation with total magnetic energy.